

Experimental Validation of the Interfacial Form of the Wiedemann-Franz Law

R. B. Wilson and David G. Cahill

*Department of Materials Science and Engineering, and Frederick Seitz Materials Research Laboratory,
University of Illinois, Urbana, Illinois 61801, USA*

(Received 15 March 2012; revised manuscript received 16 May 2012; published 19 June 2012)

The thermal conductivity of four Pd/Ir metal multilayers of total thickness 390 nm with 40, 80, 120, and 200 Pd/Ir interfaces are measured at temperatures between 78 and 295 K using time-domain-thermoreflectance. The thermal interface conductance G of the Pd/Ir interface is derived from the differences in thermal conductivity between the multilayers. A comparison of G to previously reported data for the electronic specific resistance of the Pd/Ir interface at 4 K supports the validity of the interfacial form of the Wiedemann-Franz law. The Lorenz number deduced from this comparison is within 10% of the Sommerfeld value at all temperatures, well within the experimental uncertainties of $\approx 20\%$.

DOI: [10.1103/PhysRevLett.108.255901](https://doi.org/10.1103/PhysRevLett.108.255901)

PACS numbers: 65.40.-b, 73.40.-c

The transport of thermal energy in nanostructured materials and devices is often impacted by interfaces [1]. The disruption in lattice periodicity at an interface causes the scattering of heat carriers, often leading to a dramatic reduction in thermal transport [2–4]. A detailed understanding of how heat carriers are impacted by interfaces is necessary to analyze heat transfer on the nanoscale.

Numerous studies of phonon-mediated heat flow across metal-dielectric and dielectric-dielectric interfaces have been reported in the past two decades [5,6]. As a result, substantial progress has been made towards both quantitatively and qualitatively understanding the impact that interfaces have on phonon transport [6]. However, in metallic systems, electrons are typically the dominant heat carrier, and the impact interfaces have on electron transport is important to understand.

Heat flow across metal-metal interfaces is also a significant issue for a number of technological applications. For example, the transport properties and thermal performance of metal multilayers have direct relevance to heat-assisted magnetic recording [7], spintronics [8], and magnetic sensors [9]. Furthermore, understanding the scattering mechanisms of electron-mediated heat flow across interfaces is critical for the emerging field of spin caloritronics which aims to manipulate spin currents and magnetization using heat currents [10,11].

Because of the technological and scientific impact of heat flow in metallic structures, there have been numerous experimental investigations of the thermal conductivity of nanostructured thin films, [12–14] and metal multilayers [15–17]. The standard approach has been to measure the thermal conductivity and in-plane electrical resistivity of a metallic thin film or metal multilayer, and derive an effective Lorenz number for the system, $L(T)$, from the ratio of these two values. Depending on how $L(T)$ compares with the Sommerfeld value of $2.45 \times 10^{-8} \Omega \text{ W K}^{-2}$, different conclusions are drawn about the contribution of electrons, phonons, and magnons to thermal transport [12,15,16], as well as

the validity of the Wiedemann-Franz (WF) law in these systems. Some studies have speculated that the WF law does not fully capture heat transport across metal-metal boundaries [14], suggesting electrons that are elastically reflected from metal-metal grain boundaries do not contribute to charge transport but still facilitate heat transport via interactions with phonons at the boundary. Numerous other experimental [17,18] and theoretical [19,20] investigations suggest electrons scatter diffusely at metal-metal interfaces, at least in the case of sputtered multilayers. For example, theoretical calculations of the specific electrical resistance of metal-metal interfaces, AR , found that allowing phase coherence in scattering of electrons between adjacent interfaces hindered agreement with experimental measurements of metal multilayers [18]. The notation of writing AR to denote the specific electrical resistance is widespread in the literature and is equivalent to taking the product of the resistance R and area A of an interface.

Gundrum *et al.* demonstrated that the temperature dependence of the thermal conductance of an Al/Cu interface is consistent with diffusive interfacial scattering, providing indirect evidence for the validity of the interfacial form of the WF law [17]. The interfacial form of the WF law [21] relates the specific electrical resistance of an interface AR and the thermal conductance per unit area G of an interface

$$\frac{GAR}{T} = L_0, \quad (1)$$

where T is temperature, and L_0 is the Sommerfeld value of the Lorenz number, $2.45 \times 10^{-8} \Omega \text{ W K}^{-2}$. G is a linear transport coefficient that relates the heat flux J crossing the interface to the temperature drop ΔT at the interface, $J = G\Delta T$.

Currently absent in the literature is a quantitative study that characterizes the impact individual metal-metal interfaces have on both electrical current and heat flow perpendicular to the interface. This current study helps fill this gap by directly comparing measured values of the fundamental interfacial transport coefficients G and AR for sputtered Pd/Ir metal multilayers. This study experimentally validates

the interfacial form of the WF law and is an important step towards a more complete understanding of electrical and thermal transport at the nanoscale.

We measured G of the Pd/Ir metal-metal interface using time-domain thermoreflectance (TDTR). These measurements were carried out on four samples that were part of a previous study by Acharyya *et al.* [22]. This previous study quantified AR of the Pd/Ir interface at 4.2 K. With the assumption that AR is independent of temperature, we find the measured values of $G(T)$ and AR of sputtered Pd/Ir interfaces to be consistent with the WF law for interfaces within experimental uncertainties. The measured values correspond to a Lorenz number that is within 10% of the Sommerfeld value of $2.45 \times 10^{-8} \Omega \text{ W K}^{-2}$ at all temperatures.

Measurements of the current-perpendicular-to-plane total specific resistance of sputtered Pd/Ir multilayers were previously reported by Acharyya *et al.* [22]. They found the specific electrical resistance for the Pd/Ir interface is $AR = 0.51 \pm 0.03 \text{ f}\Omega \text{ m}^2$. The specific electrical resistance of the four multilayer samples used in our TDTR study was remeasured prior to our experiments to ensure the electrical properties had not changed significantly since the original electrical measurements. Details concerning sample preparation and experimental methods used to measure the specific electrical resistance of the Pd/Ir interfaces have also been reported previously [23].

The geometry of the metal multilayers is shown in Fig. 1. We measured the layer thicknesses of each sample using picosecond acoustics [Fig. 1(b)]. The Nb and Cu thicknesses of 150 and 5 nm that we specify correct the values of 100 and 10 nm given by Acharyya *et al.* These corrections were confirmed by rechecking the original lab notebooks at Michigan State University that recorded the sputter deposition conditions for these samples. Because the electrical measurements reported by Acharyya *et al.* were made at 4.2 K, where both the Nb and Cu (due to the proximity effect) are superconducting, these corrections do not affect their data or analysis. The correct Nb thickness is, however, important for our analysis.

The effective thermal conductivity of Pd/Ir multilayers was measured using time-domain thermoreflectance (TDTR). TDTR is a well-established optical pump-probe technique that measures the evolution of surface temperature with picosecond time resolution. TDTR uses a train of short pulses from a mode-locked Ti:sapphire laser that are split into pump and probe beams. The pump beam is used to heat the sample, while the temperature evolution of the surface is monitored by measuring small, temperature-induced changes in the intensity of the probe beam reflected from the sample surface.

The heat current is not directly measured in a TDTR experiment. Instead, the TDTR approach is based on measuring how the temperature of the surface evolves as a function of time as heat flows from the top Nb layer, through

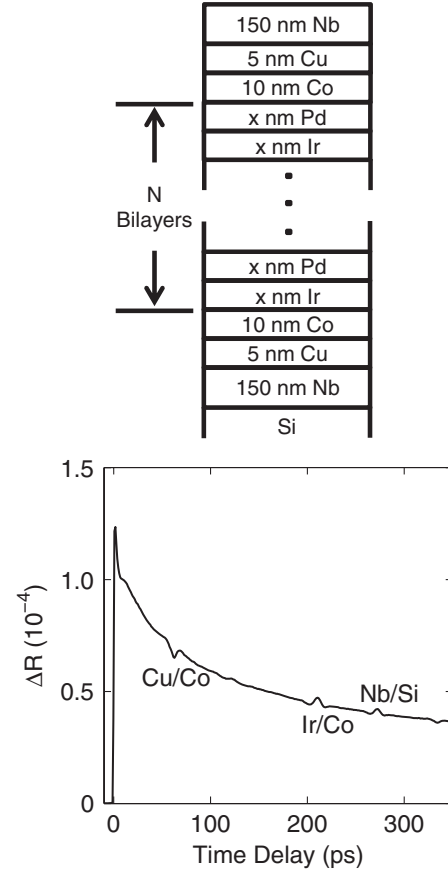


FIG. 1. (a) Geometry of metal multilayer samples. (b) Picosecond acoustics data of a 40 bilayer Pd/Ir sample. The y-axis is the change in the reflectivity of the top Nb film that is created by heating and acoustic waves generated by the pump. The x-axis is the delay time between pump and probe. The acoustic echoes are labeled by the interface that partially reflects the longitudinal acoustic wave generated by the pump.

the Pd/Ir multilayer, through the bottom Nb contact, and into the Si substrate. The thermal conductivity of the metal multilayer strongly affects the rate of thermal transport out of the top Nb film surface and therefore strongly affects its temperature evolution. We use an analytical solution to the heat diffusion equation in cylindrical coordinates to extract the thermal conductivity of the Pd/Ir multilayer [24]. The full thermal model includes parameters for the thermal conductivity, specific heat, and thickness of each layer in the sample. All input parameters for the thermal model are fixed from literature values or separate measurements (described below), except for the effective thermal conductivity of the metal multilayer. This value is determined by obtaining a best fit between the prediction of the thermal model and the experimental TDTR data. Uncertainty in the measured multilayer thermal conductivity is derived from uncertainties in the input parameters to the thermal model, and the sensitivity of the model to those parameters [17]. Further details of our experimental method and setup are described elsewhere [24,25].

Instead of entering the Cu, Co, Pd, and Ir as separate layers in the thermal model, we treat the 390 nm thick metal multilayer as one layer with a uniform effective heat capacity and a uniform effective thermal conductivity that includes the thermal resistance from the metal layers and metal-metal interfaces. The thermal conductivities used in the modeling are summarized in Fig. 2. The heat capacities at the 5 temperatures of 80, 115, 155, 207 and 298 K are 1.72, 2.22, 2.66, 2.78, and 2.98 J cm³ K⁻¹, respectively. The conductance of the Nb/Si interface was not precisely known and instead estimated. The Nb/Si interface conductance was assumed to have a value of 150 MW m⁻² K⁻¹ at room temperature, and display the same temperature dependence as the heat capacity of Nb. This value and temperature dependence is characteristic to most sputtered metal-dielectric interfaces [5,6]. The exact value for the Nb/Si interface conductance is not critical as the sensitivity of the thermal model to this interface is small—at room temperature, a 40% error in the value of

the interface conductance will cause a 1% error in the effective thermal conductivity of a multilayer.

Our estimate of the thermal conductivity of the Nb film is based on the electrical resistivity of the Nb film and the WF law. The electrical resistance of the Nb film was measured at room temperature using a four-point probe and found to be $19.6 \pm 1.4 \mu\Omega$ cm, corresponding to a residual resistivity, ρ_r , of $4.9 \mu\Omega$ cm. We assume the thermal resistance in the Nb film arises from a temperature independent electron-defect scattering rate and temperature dependent electron-phonon scattering rate. We also assume the scattering rate from electron-phonon interactions in the film is equal to the electron-phonon scattering rate in defect-free single crystal bulk Nb. The WF law suggests the specific thermal resistance of the Nb film from the electron-defect scattering will be proportional to ρ_r/L_0T , while our second assumption implies that the specific thermal resistance from the electron-phonon scattering will be proportional to $\rho(T)/(L(T)T)$, where $L(T)$ is the ratio of electrical resistivity to thermal conductivity for defect-free-bulk Nb [26], and $\rho(T)$ is the electrical resistivity of defect-free-bulk Nb [26]. These two thermal resistances will add in series. The thermal conductivity of the Nb films can then be expressed as

$$\Lambda^{\text{Nb}} = \left[\frac{\rho_r}{L_0 T} + \frac{\rho(T)}{L(T) T} \right]^{-1}. \quad (2)$$

This equation assumes that defects in the Nb film will not strongly modify the function $L(T)$. We cannot be confident of the accuracy of this assumption, as defects can alter phonon lifetimes, thereby altering the electron-phonon scattering rate. We expect elastic scattering by defects to reduce the difference between $L(T)$ and L_0 , causing Eq. (2) to converge towards the WF law. The WF law predicts a thermal conductivity that deviates a maximum of 10% from the value predicted by Eq. (2) at 80 K. Uncertainty in the measured Nb resistivity introduces further uncertainty in the Nb thermal conductivity. Weighing these two factors, we assign a high uncertainty of 10% to the thermal conductivity of the Nb when calculating the uncertainty in the metal multilayer's thermal conductivity. This is the primary source of uncertainty in our result.

The effective thermal conductivities of the Pd/Ir multilayers as measured by TDTR are shown in Fig. 2 as a function of temperature and number of interfaces. To derive the thermal conductance of the Pd/Ir interface, we assume the scattering from one interface is not coherent with scattering from an adjacent interface and that electron-phonon and electron-defect scattering rates are not significantly modified by the interfaces. This second assumption is equivalent to stating that Matthiessen's rule applies for scattering from defects, phonons, and interfaces. We believe that this is a valid assumption as long as the interface density is not so high as to create a significant modification of the band structure [27]. These assumptions

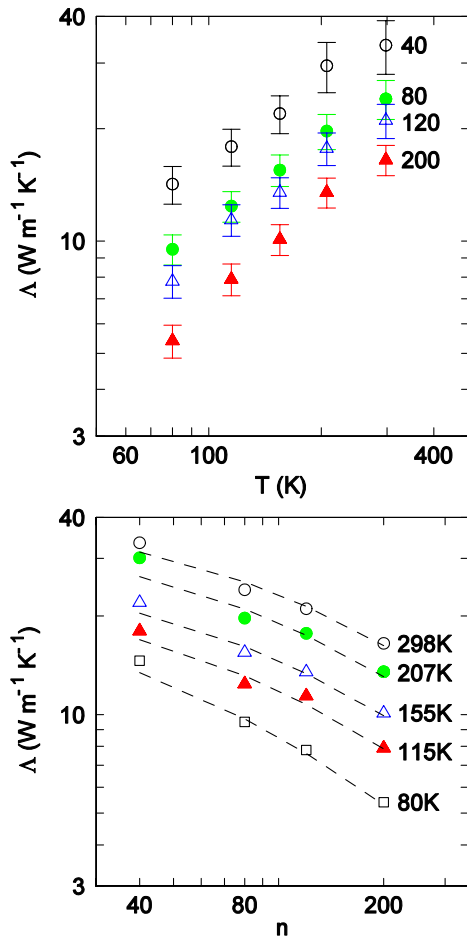


FIG. 2 (color online). Thermal conductivity of Pd/Ir samples with $n = 40, 80, 120$, and 200 interfaces plotted (a) as a function of temperature, and (b) as a function of n at selected temperatures. The dashed lines represent the best fit of the data to Eq. (3). The change in thermal resistance as a function of n yields the interfacial contribution to the thermal conductance.

imply that for a constant heat flux, the gradient of the temperature within each layer is independent of layer thickness and that the temperature drop at each interface is also independent of layer thickness. This suggests a simple relation between multilayer thermal conductivity and thermal conductance of the Pd/Ir interface:

$$R_{\text{total}}(n) = \frac{390 \text{ nm}}{\Lambda_{\text{ML}}(n)} = R_0 + \frac{n}{G_{\text{Pd/Ir}}}, \quad (3)$$

where R_{total} is the total thermal resistance of a metal multilayer, Λ_{ML} is the effective multilayer thermal conductivity, R_0 is the multilayer thermal resistance sans Pd/Ir interfaces, and n is the number of Pd/Ir interfaces in the sample. The electrical resistance analog of Eq. (3), which requires similar assumptions to derive [28], successfully describes the specific electrical resistance as a function of interfaces for a large variety of metal multilayer samples [18,22].

The thermal conductance of the Pd/Ir interface is plotted as a function of temperature in Fig. 3. At room temperature the thermal conductance of the Pd/Ir interface is $14 \pm 3 \text{ GW m}^{-2} \text{ K}^{-1}$ —the largest thermal interface conductance ever measured (the previous maximum thermal conductance of $4 \text{ GW m}^{-2} \text{ K}^{-1}$ was for an Al/Cu interface [17]). Using the interfacial form of the WF law [Eq. (1)], we derive the expected thermal interface conductance as a function of temperature using $AR = 0.51 \text{ f}\Omega \text{ m}^2$. In this derivation, we assume the interface specific resistance is independent of temperature; the value of AR of these samples has only been measured at 4.2 K. Previous experimental studies of specific electrical resistance of

metal-metal interfaces suggest AR is usually only weakly temperature dependent between 4.2 and 293 K [18].

The diffuse mismatch model (DMM) for thermal interface conductance is a commonly used tool for explaining the magnitude of phonon-mediated thermal conductance. For electron-mediated transport [17] the DMM takes the form

$$G = \frac{Z_1 Z_2}{4(Z_1 + Z_2)}, \quad (4)$$

where Z_i is given by the product of the electronic heat capacity per unit volume γT and the Fermi velocity v_f of side i ; $Z = \gamma v_f T$. This form of the DMM for electrons assumes the metals to be a degenerate electron gas. We further assume an electronic density of states independent of temperature and use low temperature measurements of γ for both Pd and Ir. The Pd and Ir films have (111) texture; therefore, we use the average Fermi velocity in the [111] direction, calculated from the electronic energy dispersion relations [29,30]. Then, $Z_{\text{Pd}} = 0.46$, $Z_{\text{Ir}} = 0.3$, and $G = 0.041 \text{ T}$, where Z and G are in units of $\text{GW m}^{-2} \text{ K}^{-1}$. The DMM result for the Pd/Ir thermal interface conductance is shown in Fig. 3. As is the case with the Al/Cu interface [17], the DMM for electrons does an excellent job describing the interface conductance, particularly considering the simplicity.

In summary, we report the thermal interface conductance of sputtered Pd/Ir interfaces between 78 and 300 K. By comparing these values to previous measurements of the specific electrical resistance of the same samples (measured by Acharya *et al.*), we provide direct experimental evidence for the validity of the interfacial form of the WF-law for metal-metal interfaces.

We thank J. Bass and W.P. Pratt, Jr., as well as R. Acharyya and H. Y. T. Nguyen who grew the multilayers, for providing to us with four of the Pd/Ir multilayers used in their study of the Pd/Ir interface specific electrical resistance [22]. This work was supported by the U.S. Department of Energy Office of Basic Energy Sciences, under Grant No. DE-FG02-07ER46459 and was carried out in the Laser and Spectroscopy Laboratory of the Materials Research Laboratory at the University of Illinois Urbana Champaign. R.B. Wilson was partially supported by a Department of Defense NDSEG fellowship during this work. We acknowledge Grant No. DMR0804126 from the NSF and the Korea Institute for Science and Technology which supported Acharyya and H. Y. T. Nguyen while preparing these samples.

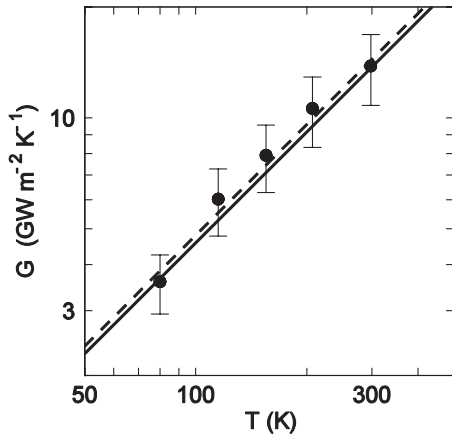


FIG. 3. Thermal conductance of the Pd/Ir interface as a function of temperature. Filled circles are derived from the time-domain thermoreflectance (TDTR) measurements shown in Fig. 2(b). The dashed black line gives the expected value of the thermal interface conductance using the interfacial form of the Wiedemann-Franz law and a temperature independent value of $0.51 \text{ f}\Omega \text{ m}^2$ for the specific electrical resistance, and the solid line gives the prediction of the diffuse-mismatch-model (DMM) for electrons based on an estimate of the Fermi velocity and density of states for Pd and Ir.

- [1] D. G. Cahill, W. K. Ford, K. E. Goodson, G. D. Mahan, A. Majumdar, H. J. Maris, R. Merlin, and S. R. Phillpot, *J. Appl. Phys.* **93**, 793 (2003).
- [2] Y. K. Koh, Y. Cao, D. G. Cahill, and D. Jena, *Adv. Funct. Mater.* **19**, 610 (2009).

- [3] V. Rawat, Y.K. Koh, D.G. Cahill, and T.D. Sands, *J. Appl. Phys.* **105**, 024909 (2009).
- [4] A. Chernatynskiy, R.W. Grimes, M.A. Zurbuchen, D.R. Clarke, and S.R. Phillpot, *Appl. Phys. Lett.* **95**, 161906 (2009).
- [5] R.J. Stevens, A.N. Smith, and P.M. Norris, *J. Heat Transfer* **127**, 315 (2005).
- [6] R.M. Costescu, M.A. Wall, and D.G. Cahill, *Phys. Rev. B* **67**, 054302 (2003).
- [7] T.W. McDaniel, *J. Phys. Condens. Matter* **17**, R315 (2005).
- [8] J. Bass and W.P. Pratt, Jr., *J. Phys. Condens. Matter* **19**, 183201 (2007).
- [9] J.M. Daughton, *J. Magn. Magn. Mater.* **192**, 334 (1999).
- [10] J. Sinova, *Nature Mater.* **9**, 880 (2010).
- [11] J. Xiao, G.E.W. Bauer, K. Uchida, E. Saitoh, and S. Maekawa, *Phys. Rev. B* **81**, 214418 (2010).
- [12] F. Völklein, H. Reith, T.W. Cornelius, M. Rauber, and R. Neumann, *Nanotechnology* **20**, 325706 (2009).
- [13] S. Yoneoka, J. Lee, M. Liger, G. Yama, T. Kodama, M. Gunji, J. Provine, R.T. Howe, K.E. Goodson, and T.W. Kenny, *Nano Lett.* **12**, 683 (2012).
- [14] Q.G. Zhang, B.Y. Cao, X. Zhang, M. Fujii, and K. Takahashi, *Phys. Rev. B* **74**, 134109 (2006).
- [15] W.H. Soe, T. Kaizuka, R. Yamamoto, and T. Matsushashi, *J. Magn. Magn. Mater.* **126**, 457 (1993).
- [16] Y. Yang, J.G. Zhu, R.M. White, and M. Asheghi, *J. Appl. Phys.* **99**, 063703 (2006).
- [17] B.C. Gundrum, D.G. Cahill, and R.S. Averback, *Phys. Rev. B* **72**, 245426 (2005).
- [18] W.P. Pratt, Jr and J. Bass, *Appl. Surf. Sci.* **256**, 399 (2009).
- [19] A. Shpiro and P.M. Levy, *Phys. Rev. B* **63**, 014419 (2000).
- [20] G.E.W. Bauer, K.M. Schep, K. Xia, and P.J. Kelly, *J. Phys. D* **35**, 2410 (2002).
- [21] G.D. Mahan and M. Bartkowiak, *Appl. Phys. Lett.* **74**, 953 (1999).
- [22] R. Acharyya, H. Y. T. Nguyen, R. Loloe, W. P. Pratt, Jr., J. Bass, S. Wang, and K. Xia, *Appl. Phys. Lett.* **94**, 022112 (2009).
- [23] S.F. Lee *et al.*, *Phys. Rev. B* **52**, 15 426 (1995).
- [24] D.G. Cahill, *Rev. Sci. Instrum.* **75**, 5119 (2004).
- [25] K. Kang, Y.K. Koh, C. Chiritescu, X. Zheng, and D.G. Cahill, *Rev. Sci. Instrum.* **79**, 114901 (2008).
- [26] R.K. Williams, W.H. Butler, R.S. Graves, and J.P. Moore, *Phys. Rev. B* **28**, 6316 (1983).
- [27] J. Bass, *Adv. Phys.* **21**, 431 (1972).
- [28] K.M. Schep, J.B.A.N. van Hoof, P.J. Kelly, G.E.W. Bauer, and J.E. Inglesfield, *Phys. Rev. B* **56**, 10 805 (1997).
- [29] F.M. Mueller, A.J. Freeman, J.O. Dimmock, and A.M. Furdyna, *Phys. Rev. B* **1**, 4617 (1970).
- [30] S.P. Hörnfeldt, L.R. Windmiller, and J.B. Ketterson, *Phys. Rev. B* **7**, 4349 (1973).